

Linking the West African monsoon's onset with atmospheric circulation patterns

PATRICK LAUX¹, HARALD KUNSTMANN¹ &
ANDRÁS BÁRDOSSY²

¹ *Institute for Meteorology and Climate Research (IMK-IFU), Forschungszentrum Karlsruhe, D-82467 Garmisch-Partenkirchen, Germany*
patrick.laux@imk.fzk.de

² *Institute for Hydraulic Engineering, University of Stuttgart, D-70569 Stuttgart, Germany*

Abstract Particularly in regions where precipitation is limited to only a few months per year, the reliable determination of the rainy season's onset and thus the start of the sowing time on a daily basis is of crucial importance for sustainable water management and food production. A fuzzy-logic based definition for the major rainy season's onset on a regional scale has been developed using ground-measured rainfall information. The definition accounts for the most important agricultural aspects. Further, this study presents a methodology, which is conditioning the single event "onset of the rainy season" to daily large-scale atmospheric circulation via automated objective classification of atmospheric circulation patterns based on fuzzy rules. This study has been carried out within a sector from 40°W to 30°E and 10°S to 60°N, covering a large area of the North Atlantic for atmospheric circulation analysis, and, for sea surface temperature, a sector from 30°W to 10°E and 20°S to 0°. These fuzzy rules are obtained using a simulated annealing optimization of the classification performance. A bootstrapping resampling scheme is applied in order to check the significance of the results. Sensitive predictor variables, with regard to the onset of the rainy season in West Africa, as well as their spatial patterns, are presented and discussed. The aim is for an overall integration in a hydro-meteorological Decision Support System (DSS).

Key words Volta basin; West Africa; rainy season onset; objective circulation patterns; simulated annealing; occurrence probability

INTRODUCTION

Of all the climatic factors in tropical areas, precipitation variability is seen to be the most critical factor for rain-fed agriculture and thus for ensuring food security. In West Africa, life revolves around the occurrence or non-occurrence of rainfall and its spatial and temporal distribution (Sivakumar, 1992). The seasonal cycle of the general atmospheric circulation is the most regular element of interannual precipitation variations. The onset of the rainy season, which is seen to be the most important factor in agricultural planning (Steward, 1991), is strongly affected by the movement of the Intertropical Convergence Zone (ITCZ). The ITCZ is a boundary between the two Hadley-type cell circulations of the two hemispheres. The displacement of the ITCZ in West Africa is amplified by the transition of the great northern-winter dry season (occurrence of the Harmattan as far as the Guinean coast) and the northern-summer rainy season (southwesterly monsoonal flow advects the water vapour for rainfall production) (Fontaine, 1991). According to Sultan & Janicot (2003), the West African monsoon onset dynamic follows two distinct phases, the pre-onset and the onset phase.

The pre-onset occurs in late spring when the (ITCZ) establishes itself at 5°N (~14 May), whereas the actual onset occurs when the ITCZ shifts abruptly northwards (~24 June). Then, the ITCZ moves from 5° to 10°N, where it stays for the whole of August. Following the movement of the ITCZ, the monsoon is of bimodal character in the Guinea region and of single mode in the Sahel zone. In these zones, the rainy season's onset seldom occurs abruptly and is often preceded by short isolated showers with intermittent dry spells of various lengths, which are often misinterpreted as the start of the rainy season. The mean West African boreal summer circulation has been described by various authors (e.g. Hastenrath, 2000; McGregor & Nieuwolt, 1998). The wet southwesterly flow moves into the inner continent as a function of pressure and thermal gradients that settle between the relatively cool ocean and the heated desert. In the upper layers, there are two prevailing wind systems: the African Easterly Jet (AEJ) at approximately 600 hPa and the Tropical Easterly Jet (TEJ) at 150 hPa. The strength of both plays a major role for abnormally drought and wet conditions (Jenkins *et al.*, 2002). Intensified magnitudes of the AEJ are accompanied by a weakened monsoonal flow and therefore dry conditions, whereas a stronger TEJ is associated with wet conditions. Additional to this influence of the upper-layer wind fields, minor total rainfall amounts are associated with: (a) an enhancement of the Azores anticyclone and a weakening of the St Helena anticyclone linked with an increase of the sea surface temperature (SST) of the equatorial and south subtropical Atlantic Ocean, a decrease of the SST in the Northern Atlantic Ocean and a more southward position of the ITCZ (Lambergson, 1977), and (b) positive sea-level pressure anomalies (SLPA) over the northeast Atlantic.

The following section of this paper will cover data availability and a description of the methodology. Results are then summarized in the third section and finally, the conclusions are drawn.

DATA AND METHODOLOGY

Data

For the statistical analyses, daily precipitation time series from Burkina Faso and Ghana were used. The meteorological data were obtained from the Institut National de l'Environnement et des Recherches Agricoles (INERA) at Ouagadougou (Burkina Faso), the Meteorological Service of Burkina Faso in Ouagadougou and the Meteorological Service Department in Accra (Ghana). The data were quality checked by the Ghanaian and Burkinabé meteorological services. Due to large data gaps within most of the observation time series, only a limited number of the available meteorological observation stations could be used.

Figure 1 (left) shows the two domains of the classification scheme and the spatial distribution of the synoptic meteorological stations used, which offered continuous daily rainfall data from 1961 to 1999 (right). Preliminary studies, correlating monthly areal precipitation (CRU data from 1901–1996; New *et al.*, 2000) of the Volta basin (1°W to 3°E and 5°N to 12°N) with global gridded SLP and SST fields showed significant patterns in the Mediterranean area and North Atlantic, i.e. around the onset of the rainy season (not shown here), resulting in the extensions of the domain to

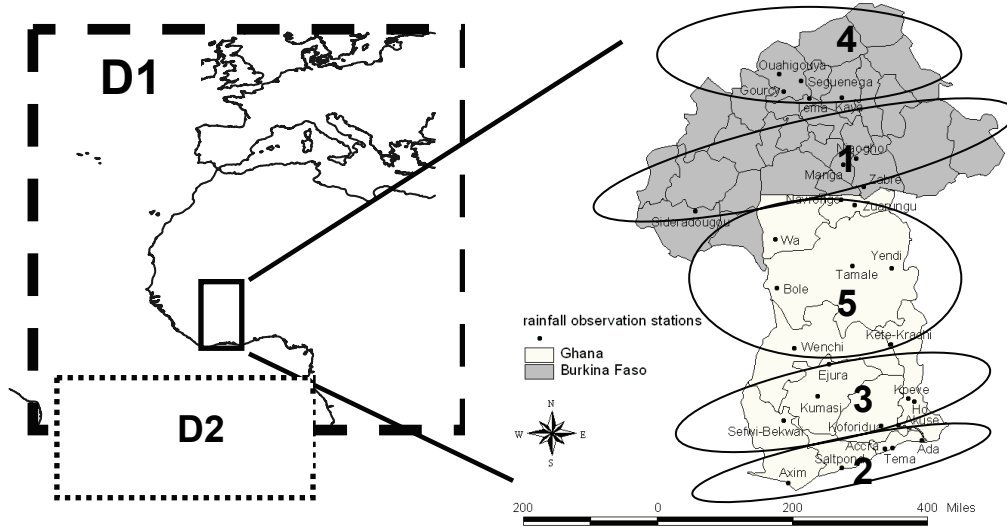


Fig. 1 Domains for the Circulation Pattern Analysis (left) and spatial distribution of areas with similar rainfall behaviourism within the Volta basin, represented through five ellipses (right).

60°N. Five sub-regions within the Volta basin are analysed in terms of precipitation variability. These sub-regions correspond to areas with different rainfall characteristics and are subsequently referred to as PC1–PC5. The NCEP re-analysis data are chosen as a principle data set for atmospheric parameters. NCEP re-analysis data are produced in a joint effort between the National Center for Environmental Prediction (NCEP) and the National Center for Atmospheric Research (NCAR). The re-analysis data are classified into four classes due to the relative influence of: (1) the observational data, and (2) the model on the gridded fields. *Class A* indicates the most reliable class of variables: the analysis variable is strongly influenced by the observed data. *Class B* is the next most reliable class of variables. Although some observational data directly affect the value of the variable, the model also has a very strong influence on the output values. *Class C* represents the least reliable class of variables, where no observations directly affect the output, and it is derived solely from the model computations, forced by the model's data assimilation process. *Class D* fields are fields containing fixed values. The roughness length and land–sea mask are examples for Class D. The data were retrieved from the NOAA-CIRES Climate Diagnostics Center (CDC) webpage (<http://www.cdc.noaa.gov/cdc/reanalysis/reanalysis.shtml>) with a temporal resolution of six hours and a spatial resolution of 2.5°. Table 1 presents the re-analysis fields used and their classification.

Three additional fields, referred as moisture flux have been calculated using specific humidity (SH) and the U- and V-component of wind at the 500, 600 and 850 hPa level:

$$MF_UV(lv) = SH(lv) \times \sqrt{U(lv)^2 + V(lv)^2} \quad (1)$$

$$MF_U(lv) = SH(lv) \times U(lv) \quad (2)$$

$$MF_V(lv) = SH(lv) \times V(lv) \quad (3)$$

where lv denotes the atmospheric level in hPa.

Table 1 Utilized re-analysis fields and their quality classification. Over land and sea ice, the skin temperature is a prognostic variable. Over open water, the skin temperature is fixed at its initial value (from the Reynolds SST data). The Reynolds SST analyses were done weekly and the reconstructed SST done monthly. The analyses were linearly interpolated to daily values.

Variable	Abbreviation	Level	Class
Sea level pressure	SLP	Surface	A
Skin temperature	SST	Surface	B
v-component of wind	U	300 hPa, 500 hPa, 700 hPa	A
u-component of wind	V	300 hPa, 500 hPa, 700 hPa	A
Specific humidity	SH	500 hPa, 850 hPa, 1000 hPa	B
Geopotential height	GEO POT	500 hPa, 850 hPa	A

Methodology

The first part of the methodology section is an objective classification of daily circulation patterns for various atmospheric fields of the past climate (1961–1999). It has been successfully applied for statistical downscaling of precipitation and temperature features, especially for Central Europe (Bárdossy *et al.*, 1995, 2002; Panagoulia *et al.*, 2006). The challenging part of this work is to apply this methodology to a single event, namely the onset of the rainy season, and for an area in which the rainfall behaviour is not yet fully understood due to the complexity of its influencing factors. Secondly, a fuzzy-logic based definition (Laux *et al.*, 2006) has been applied to calculate the rainy season onset dates for five regions within the Volta basin. A five-day period (± 2 days around the onset date) and two further classes (dry and wet) with different weights (class values) are then linked to the large-scale circulation patterns. Third, a frequency analysis is performed in combination with a bootstrapping scheme to assist detection of the patterns that are most responsible for the onset of the rainy season. A brief description of the method is presented in the following subsections.

Fuzzy rule-based classification of circulation patterns The fuzzy-rule based classification is described in Bárdossy *et al.* (1995). Here, only a brief description is given. As a first step, the $2.5^\circ \times 2.5^\circ$ NCEP re-analysis fields are transformed to standardized anomalies by subtracting the long-term mean and dividing the difference by the long-term standard deviation:

$$g(i,t) = \frac{h(i,t) - h(i,t')}{\sigma(i,t')} \quad (4)$$

where $h(i,t)$ is the observed variable at grid point i and time t ; $h(i,t')$ is the mean and $\sigma(i,t')$ the standard deviation of the variable at grid point i over the annual cycle.

The daily anomalies $\sigma(i,t)$ are then classified into the categories: (1) high $(0.2, 1.0, \infty)_T$; (2) medium high $(0, 0.6, 1.4)_T$; (3) medium low $(-1.4, -0.6, 0)_T$; (4) low $(-\infty, -1, -0.2)$; and (5) indifferent for the circulation patterns using triangular fuzzy membership functions (subscript T). Usually most of the grid-points belong to class number 5, since only characteristic ones are assigned to other classes. For a given time t and location i , the membership corresponding to rule k is defined as:

$$\mu_{i,k} = \mu_{v(i)}^k(g(i,t)) \quad (5)$$

Thus, a circulation pattern CP_k is fully characterized by an index vector $v(k) = \{v(1)^k \dots v(n)^k\}$, which defines the location of the five anomaly classes in the target area. After that, classification of daily fields is carried out by calculating the degree of fulfilment (DOF) for each rule based on the membership values μ :

$$DOF(k,t) = \prod_{l=1}^4 \left(\frac{1}{N(v(i)^{(k)} = l)} \sum_{v(i)^{(k)}=l} \mu(i,k)^{P_l} \right)^{\frac{1}{P_l}} \quad (6)$$

where N is the number of grid points classified as class l , and P_l is a parameter, which is modifying the influence of selected classes towards the DOF .

Finally, the rule k , where $DOF(k,t)$ is maximal, is selected as the CP for the day t and the result is a vector with one objective circulation pattern per selected day.

Deriving a suitable objective function for optimization procedure due to regional onset of the rainy season in the Volta basin The onset dates of the rainy season for the years 1961–1999 were computed using fuzzy-logic based definition, as described in Laux *et al.* (2006). It is a modified definition from Stern *et al.* (1981), and the onset is regarded as the first date after 1 March, with:

- (1) occurrence of five consecutive days in which at least 25 mm of rain fall;
- (2) the start day and at least two other days in this 5-day period are wet (at least 0.1 mm rainfall recorded);
- (3) No dry period of seven or more consecutive days occurs in the following 30 days.

As all the constraints have to be fulfilled simultaneously, this approach delivers onset dates that are too late to be reasonable within the Volta basin, and the following modification has been performed. Each definition constraint is attached to a fuzzy membership function (Fig. 2). Then the onset date is defined as the first day of year where the product μ of the three membership grades (μ_1, μ_2, μ_3) exceeds a defined threshold value. A threshold value of 0.4 was found via trial and error to deliver realistic results for the whole Volta basin. A vector containing the timing of the rainy season's onset has been built up, including two further classes: a period with respective dry and wet conditions and the start of the rainy season. Table 2 presents the classes and their occurrence with respect to the calculated onset of the rainy season.

Table 2 Classification to build up a class vector for each day during the time period 1 March–31 October.

Class	Time period	Value
Dry	40 to 3 days before the onset	0
Onset	2 days before to 2 days after the onset date	100
Wet	3 to 40 days after the onset	2

All other days of year were assigned to “–9” and thus excluded from the calculations. Two types of objective function were defined. The first one deals with the probability of the occurrence of each class on a given day:

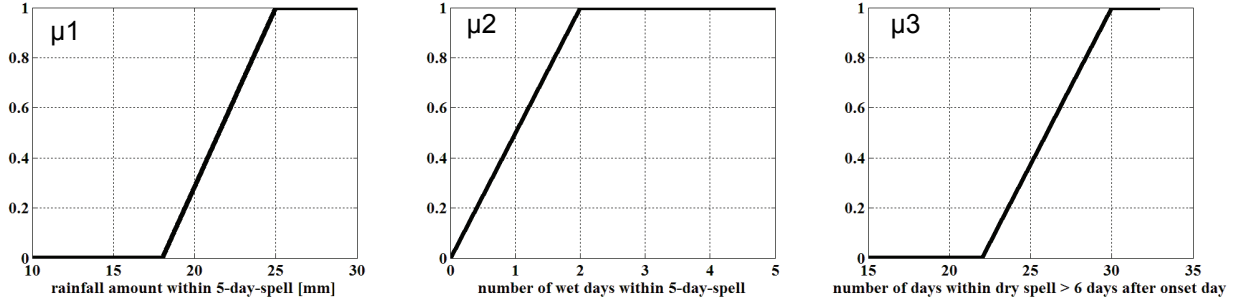


Fig. 2 Membership functions representing the three definition constraints. The first day of year, where the product of all three membership grades μ_1 , μ_2 and μ_3 exceeds the value 0.4 is regarded as the onset of the rainy season.

$$O_i = \sum_{i=1}^S \sqrt{\frac{1}{T} \sum_{i=1}^T (p(CP(t))_i - \bar{p}_i)^2} \quad (7)$$

where S is the number of stations within a region with rainfall observations, T is the number of days in the time series and $p(CP(t))_i$ is the CP-conditional probability of the class occurrence at station i within one region. A second objective function was introduced to focus the onset of the rainy season with its class value “100”:

$$O_2 = \sum_{i=1}^S \frac{1}{T} \sum_{i=1}^T \left| \left(\frac{z(CP(t))_i}{\bar{z}_i} \right)^{1.5} \right| \quad (8)$$

where \bar{z}_i is the overall average of the class values at station i within one region. High values of O_2 indicate that the conditional class amount of a CP differs clearly from the average value. Optimization was performed using the simulated annealing algorithm (Press *et al.*, 1992; Salamon *et al.*, 2000) and the sum of O_1 and O_2 as overall objective function O . The optimization starts with an arbitrary set of fuzzy rules, which classifies the daily anomalies of the re-analysis field into a CP time series, determines $p(CP)$ and $z(CP)$ by frequency analysis and calculates the overall objective function O . Then a rule is randomly selected and one of the five categories v is randomly assigned to a randomly chosen grid point. A new classification is performed and O is calculated again. If O exceeds the corresponding value of the old classification, then the change is accepted. If not, the change is accepted with a probability that decreases exponentially with decreasing annealing temperature. More details on the optimization scheme are given in Bárdossy *et al.* (2002).

Judging the quality of the classification To shed light on the onset class, a special onset parameter which consists of the ratio of conditional probability at the onset of the rainy season (days classified as “100”) and the conditional occurrence probabilities for all classes has been calculated:

$$O_{p(ONSET)} = \frac{p_{i(ONSET)}(CP)}{p_i(CP)} \quad (9)$$

After classification, the *CP* with the largest value for $O_{p(ONSET)}$ is obtained for all analysed predictors in the five distinct regions at the different atmospheric levels, respectively. Next, 500 bootstraps holding the same occurrence probabilities as the original *CP* time series were generated and the $O_{p(ONSET)}$ was calculated for each realization. If $O_{p(ONSET)}$ of no realization exceeds its value as determined from the original time series, which has to be located simultaneously outside the 3 s interval of the bootstraps, the *CP* is seen to be significant for the rainy season's onset.

RESULTS

Many circulation patterns of various predictor variables related to the onset of the rainy season in different regions within the Volta basin were found. Two examples will be highlighted subsequently. The classification scheme for the horizontal component of the moisture flux in 500 hPa separates the onset class more clearly than all other variables. Significant features could be found for the regions associated to PC1, PC3 and PC4. For the region associated to PC1 (southern Burkina Faso), CP5 is related strongly to the onset of the rainy season. Table 3 shows the relative occurrence frequency, the occurrence frequency for the onset class and the quality parameter $O_{p(ONSET)}$ for each *CP*:

Table 3 Quality measures for u-component moisture flux at 500 hPa level conditioned on onset of the rains in PC1.

MF_U(500 hPa), PC1	Rel. frequency (%)	Cond. frequency (%)	$O_{p(ONSET)}$
CP1	16.77	15.38	0.92
CP2	0.63	0.00	0
CP3	3.16	4.62	1.46
CP4	31.34	25.64	0.82
CP5	4.55	11.28	2.48
CP6	12.57	18.46	1.47
CP7	15.63	20.00	1.28
CP8	0.60	0.00	0
CP9	2.49	0.00	0
CP10	12.27	4.62	0.38

Figure 3 shows the mean normalized distribution of CP5, averaged over 1961–1999. In contrast to the mean normalized distribution of all other patterns, CP5 shows a strong positive anomaly over Egypt. Five hundred bootstraps of *CP* time series holding the same conditional occurrence probabilities were generated. Figure 4 depicts the quality criterion $O_{p(ONSET)}$ for each realization. Since $O_{p(ONSET)}$ of CP5 exceeds the values of all realizations, it can be seen to be significant. Sea surface temperature holds no significant features within Domain1. For Domain2, covering the tropical south Atlantic, SST is revealed as a suitable predictor variable for the onset of the rainy season in the coastal region (PC2). Table 4 shows the strongest relationship of CP8 with the monsoon's onset in this region.

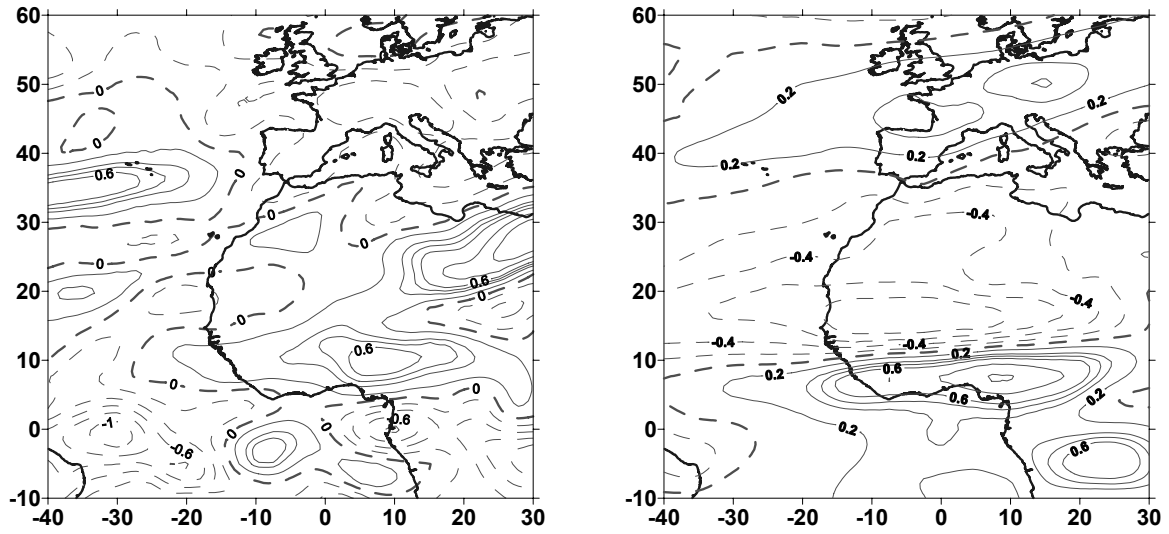


Fig. 3 Mean normalized MF-U distribution at 500 hPa of CP5 associated with the start of the rains in PC1 (left) and mean normalized MF-U distribution at 500 hPa of CP4, which is not linked to the rainy season's onset (right).

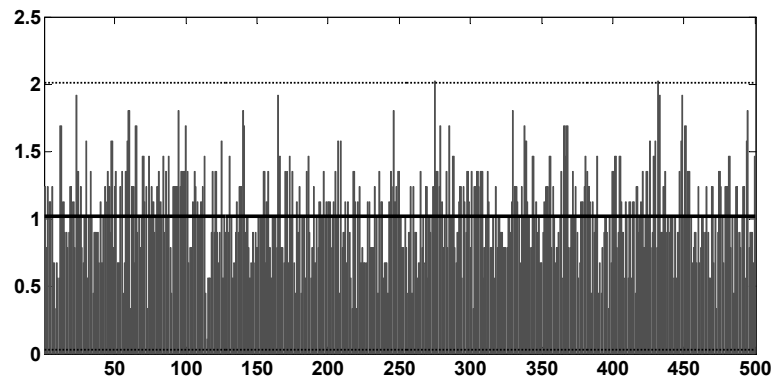


Fig. 4 Bootstrapping scheme for CP5 and MF-U at 500 hPa conditioned on the onset of the rains in PC1. 500 realizations of $O_{P(ONSET)}$ were calculated and compared to $O_{P(ONSET)}$ for CP5 (2.48). The solid line represents the mean value and the dashed line the 3 s value of $O_{P(ONSET)}$ for all realizations.

Table 4 Quality measures for SST conditioned on onset of the rains in PC2.

SST, PC2	Rel. frequency (%)	Cond. frequency(%)	$O_{p(ONSET)}$
CP1	8.21	10.53	1.28
CP2	4.57	2.63	0.58
CP3	6.92	10.00	1.45
CP4	20.30	15.26	0.75
CP5	13.20	17.37	1.32
CP6	9.02	5.26	0.58
CP7	10.68	3.68	0.35
CP8	9.50	17.89	1.88
CP9	7.02	5.26	0.75
CP10	10.58	12.11	1.14

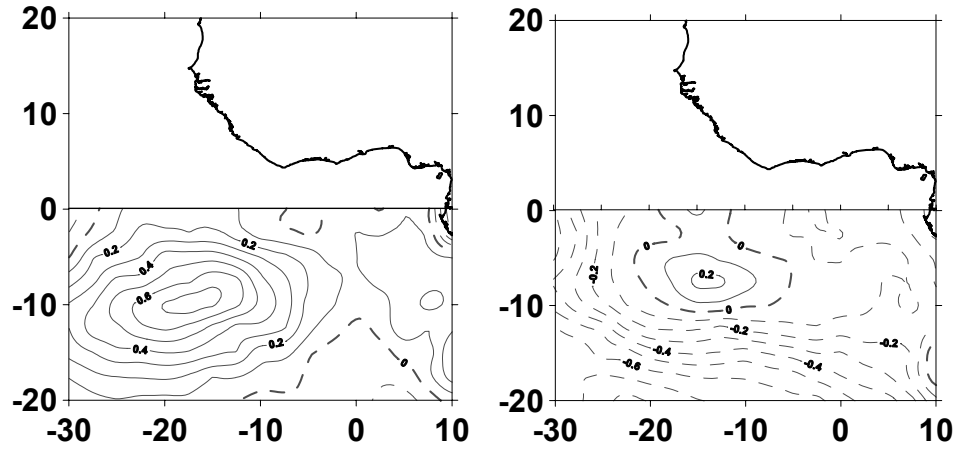


Fig. 5 Mean normalized SST distribution of CP8 associated to the start of the rains in PC2 (left), and mean normalized SST distribution of CP7, which is not linked to the rainy season's onset (right).

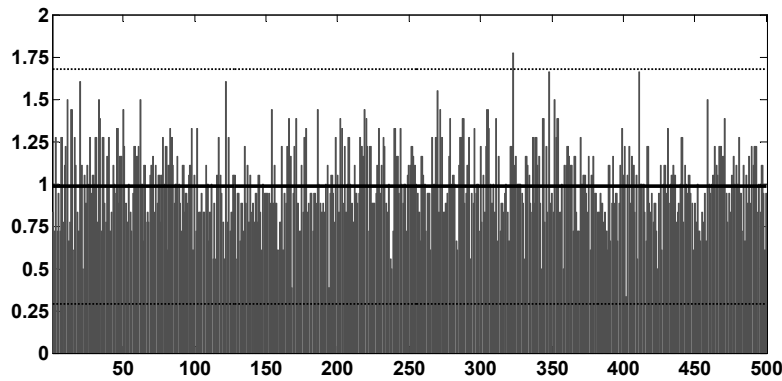


Fig. 6 Bootstrapping scheme for CP8 and SST conditioned on the onset of the rains in PC2. 500 realizations of $O_{P(ONSET)}$ were calculated and compared to $O_{P(ONSET)}$ for CP8 (1.88). The solid line represents the mean value and the dashed line the 3s value of $O_{P(ONSET)}$ for all realizations.

The mean normalized SST distribution of CP8 (Fig. 5) is offering the largest positive anomalies in the Atlantic Ocean, with a maximum value around 18°W,10°S. Figure 6 proves the significance of this pattern.

CONCLUSIONS

The fuzzy-rule based classification is a valuable methodology for linking meteorological parameters to the single event *onset of the rainy season* in the Volta basin. To the authors' knowledge, there are no comparable studies which link the single event *onset of the rainy season*, represented through a period of 5-days per year, with circulation patterns of this 5-day-period in West Africa. Due to its low demands in computational time in comparison to dynamical downscaling, it is well suited for implementation in a decision support system (DSS). Classifying daily GFS (AVN) fields of the most suitable predictors into CP classes would add probabilistic

information to decide whether the rainy season has already started. Then, this information could be broadcast via radio or television to support farmers' decisions about the optimal planting time.

Acknowledgements This work was funded by the German Ministry of Education and Science (BMBF) within the GLOWA-Volta project. Financial support is gratefully acknowledged.

REFERENCES

- Ati, O. F., Stigter, C. J. & Oladipo, E. O. (2002) A comparison of methods to determine the onset of the growing season in Northern Nigeria. *Int. J. Climatol.* **22**, 731–742.
- Bárdossy, A., Duckstein, L. & Bogárdi, I. (1995) Fuzzy rule based classification of atmospheric circulation patterns. *Int. J. Climatol.* **15**, 1087–1097.
- Bárdossy, A., Stehlik, J. & Caspary, H.-J. (2002) Automated objective classification of daily circulation patterns for rainfall and temperature downscaling based on optimised fuzzy rules. *Clim. Res.* **23**, 11–22.
- Biau, G., Zorita, E., von Storch, H. & Wackernagel, H. (1999) Estimation of precipitation by kriging in the EOF space of the sea level pressure field. *J. Clim.* **12**, 1070–1085.
- Buishand, T. A. (1977) *Stochastic Modeling of Daily Rainfall Sequences*. Veenman and Zonen, Wageningen, The Netherlands.
- Chandler, R. E. & Wheeler, H. S. (2002) Analysis of rainfall variability using generalized linear models: a case study from the west of Ireland. *Water Resour. Res.* **38**(10), 1192.
- Chin, E. H. (1977) Modeling daily precipitation process with Markov chain. *Water Resour. Res.* **13**, 949–956.
- Garbutt, D. J., Stern, R. D., Dennett, M. D. & Elston, J. (1981) A comparison of the rainfall climate of eleven places in West Africa using a two-part model for daily rainfall. *Met. Atmos. Physics* **29**, 137–155.
- Hastenrath, S. (2000) Interannual and longer term variability of upper-air circulation over the tropical Atlantic and West Africa in boreal summer. *Int. J. Climatol.* **20**, 1415–1430.
- Janicot, S. & Pocard, I. (1997) Impact of warm ENSO events on atmospheric circulation and convection over the tropical Atlantic and West Africa. *Ann. Geophysicae* **15**, 471–475.
- Jenkins, G. S., Adamou, G., & Fongang, S. (2002) The challenges of modeling climate variability and change in West Africa. *Climatic Change* **52**, 263–286.
- Kasei, C. N. & Afuakwa, J. J. (1991) Determination of optimum planting date and growing season of maize in the northern savanna zone of Ghana. In: *Soil Water Balance in the Sudan Sahelian Zone* (ed. by M. V. K. Sivakumar, J. S. Wallace, C. Renard & C. Giroux), 593–600. IAHS Publ. 199. IAHS Press, Wallingford, UK.
- Kowall, J. A., & Kassam, A. H. (1978) *Agricultural Ecology of Savanna – A Study of West Africa*. Oxford University Press, Oxford, UK.
- Laux, P., Kunstmann, H. & Bárdossy, A. (2007) Predicting the regional onset of the rainy season in West Africa. *Int. J. Climatol.* (accepted).
- McGregor, G. R. & Nieuwolt, S. (1998) *Tropical Climatology*. Wiley, Chichester, UK.
- New, M. G., Hulme, M. & Jones, P. D. (2000) Representing twentieth-century space-time climate variability. Part II: Development of 1901–1996 monthly grids of terrestrial surface climate. *J. Clim.* **13**, 2217–2238.
- Nicholson, S. E. (1994) Recent rainfall fluctuations in Africa and their relationship to past conditions over the continent. *The Holocene* **4**, 121–131.
- Omotosho, J. B., Balogun, A. A. & Ogunjobi, J. K. (2000) Predicting monthly and seasonal rainfall, onset and cessation of the rainy season in West Africa using only surface data. *Int. J. Climatol.* **20**, 865–880.
- Panagoulia, D., Bárdossy, A. & Lourmas, G. (2006) Diagnostic statistics of daily rainfall variability in an evolving climate. *Adv. Geosci.* **7**, 349–354.
- Pielke, R. A. Sr, Avissar, R., Raupach, M., Dolman, H., Zeng, X. & Denning, S. (1998) Interactions between the atmosphere and terrestrial ecosystems: Influence on weather and climate. *Global Change Biol.* **4**, 101–115.
- Palmer, T. N., Brankovic, C., Viterbo, P. & Miller, M. J. (1992) Modeling interannual variations of summer monsoons. *J. Clim.* **5**, 399–417.
- Richards, P. (1983) Ecological change and the politics of African land use. *African Studies Review* **26**, 1–72.
- Salamon, P., Sibani, P. & Frost, R. (2000) *Facts, Conjectures, and Improvements for Simulated Annealing*. SIAM Monographs on Mathematical Modeling and Computation, Philadelphia, USA.
- Sivakumar, M. V. K. (1988) Predicting rainy season potential from the onset of rains in Southern Sahelian and Sudanian climatic zones of West Africa. *Agric. For. Met.* **42**, 295–305.
- Sivakumar, M. V. K. (1992) Climate change and implications for agriculture in Niger. *Climatic Change* **20**(4), 297–312.
- Stern, R. D. & Coe, R. (1982) The use of rainfall models in agricultural planning. *Agric. Met.* **26**, 35–50.

- Steward, J. I. (1994) Utilizing rainfall probabilities referenced to crop seed germination dates to assess risk and develop response farming strategies for Asmara, Eritrea. Workshop for the famine mitigation activities support activity of USAID, US Foreign Disaster Assistance, Asmara.
- Stockenius, T. (1981) Interannual variations of tropical precipitation patterns; *Mon. Weath. Rev.* **109**, 1233–1247.
- Sultan, B. & Janicot, S. (2003) The West African monsoon dynamics. Part II: The “pre-onset” and the “onset” of the summer monsoon. *J. Clim.* **16**, 3407–3427.
- Usman, M. T. & Reason, C. J. J. (2004) Dry spell frequency and their variability over southern Africa. *Climate Research* **26**, 199–211.
- Walter, M. W. (1967) Length of the rainy season in Nigeria. *Nigerian Geogr. J.* **10**, 123–128.